SIZE-DEPENDENT OPTICAL PROPERTIES OF COPPER NANOPARTICLE OVER A WIDE RANGE OF WAVELENGTHS: AN ELECTROMAGNETIC SIMULATION STUDY

Samir Thakur[1], Dilip Saikia[2] and Nirab C. Adhikary[3]*
[1]*Physical Science Division, Department of Applied Sciences, Gauhati University, Guwahati-781014, India*
[2]*Dept. of Physics, Silapathar College, Silapathar, Dhemaji- 787059, India*
[3]*Physical Sciences Division, Institute of Advanced Study in Science and Technology, Paschim Boragaon, Garchuk, Guwahati -781035, India*
*For correspondence. (nirab_iasst@yahoo.co.in)

Abstract: In this article, we modulate the optical absorption, scattering, extinction, transmission and field intensities of an ellipsoid copper nanoparticle by tuning its dimension. The finite-difference time-domain (FDTD) method is employed for this electromagnetic simulation study and a comparative investigation has been carried out. In the investigation it is found that Cu nanoparticle with 20 nm size exhibiting the optical absorption at the resonant wavelength ~530 nm. This plasmon peak is shifted to ~550 nm when the particle size is increased to 40 nm. In addition to shifting, the enhancement of the plasmon peak is also observed. This nonlinear enhancement arises due to the size dependent property of the surface plasmon resonance (SPR). For smaller nanoparticle, the scattering is found to be negligible as compared to the larger particle. The scattering becomes dominant as the particle size increases beyond 28 nm. The scattering cross-sections of all the particle decreases at the longer wavelength. All the structures exhibit a strong transmission minimum at a wavelength close to 590 nm in the visible spectrum. However, above 600 nm high transmission is observed. The electric field intensity is also enhanced from 5.15 (V/m)2 to 16.9 (V/m)2 as the particle size increases from 20 nm to 40 nm. We strongly believe that this research could provide an overall idea about the importance of particle size variation while fabricating Cu based solar energy harvesting systems, plasmonics photovoltaic devices etc.

Keywords: FDTD; Absorption; Scattering; Extinction Cross-section; Electric and magnetic field intensity.
PACS: 61.46.+w, 61.46.−w, 61.46.Df

1. Introduction:

The localized surface plasmons resonance (LSPR) phenomenon is found to be the major factor in metal nanostructures to show the multiple optical characteristics of their bulk counterparts. Whenever electromagnetic radiation interacts with these types of nanoparticles (NPs), strong excitation within the visible or even near-infrared range is observed due to the coherent oscillations of the conduction electrons. Additionally, it provides substantial electric field enhancement within the governed resonance wavelengths [1-3]. Noble metal nanostructures offer good platforms for very sensitive optical nanosensors, photonic elements, and other applications because of their broad-spectrum response and photosensitivity [4]. In the visible as well as near-infrared (NIR) section of the spectrum, silver and gold NPs show distinct optical properties that are incredibly helpful for a variety of applications including nanoscale optical elements and systems [5] chemical as well as biomolecular sensing [6] medical imagery and photothermal treatment [7] and surface-enhanced Raman spectroscopy (SERS). Copper is another most highly used metal in electronics applications due to its higher conductivity as well as affordable price. The development of Cu based miniaturized nanodevices which integrate electronic, photonic, chemical, and biological features is extremely important for near future electronics and sensors [8]. In these nanoparticles, the position of the optical spectrum is highly sensitive to their size, shape as well as dielectric environment [9]. However, in the case of Cu, it is found that Cu can easily be oxidized in air and water medium to form cupric oxide (CuO) and cuprous oxide (Cu2O), depending on its valence state. Therefore, experimental preparation of purely Cu nanoparticles is challenging [10] and thus the LSPR property is not fully understood. In addition to that Cu NPs are predicted to be an alternate option to Au or Ag NPs because the excited resonant wavelengths of spherical Cu NPs are in close proximity to those of spherical Au NPs [11]

and also the photoelectric work function of Cu (4.65 ± 0.05 eV) located in between that of Ag (4.0 ± 0.15 eV) as well as that of Au (5.1 ± 0.10 eV) [12]. A series of research articles have already been published to investigate the plasmonic property of Cu NPs. Among those Lin et. al investigated the use of Cu NPs for highly efficient, scalable, cost-effective solar steam generation applications [13]. Katyal and co-workers investigated the plasmonic properties of Cu and other metals for nanosphere and nanorod geometrical structure by varying its particle size and found that nanorod shows a higher refractive index sensitivity (RIS) factor as compared to the nanosphere [14]. Singh et al examined the absorption improvement of GaAs solar cells with Cu nanoparticles by using the FDTD method. Their simulation outcomes revealed about 37% light absorption enhancement in comparison with bare GaAs [15]. There are a number of publications available for Cu NPs. However very few research papers have been found where the size variation of the ellipsoid geometrical structure of Cu NPs is considered to enhance the optical absorption, scattering, extinction cross-sections as well as electric field intensities. Therefore, in this work, we have varied the size of an ellipsoid Cu nanoparticle, and found that it has a major contribution to the improvement of optical cross-sections and field intensities. The absorption, scattering, extinction cross-section spectra, as well as transmission, are then simulated along with the electric and magnetic field distribution as a function of the wavelength of the incident radiation.

2. Structure design and theory:

Maxwell's four partial differential electromagnetic equations are used to simulate the optical properties and field intensities of the ellipsoid single Cu nanoparticle. The overall research of light interaction with a small metallic sphere was basically performed by Gustav Mie, in which Maxwell's equations were analytically solved and scattering as well as absorption coefficients were calculated [16] FDTD is known as probably the most well-established numerical method developed by Kane S. Yee in order to solve Maxwell's equations for the given materials having the complicated geometrical structure [17]. In this research, commercial software known as Ansys Lumerical [18] is used to investigate the optical properties of the metal nanoparticle, the same software package has been utilized widely by lots of researchers [19, 20]. In this particular method, the volume surrounding the material is subdivided into smaller cubic cells that are known as the Yee cells. The algorithm starts with some guess values, both the electric as well as magnetic fields are calculated by applying Maxwell's equations and then the first-order approximation values are examined. These values are again provided to Maxwell's equations in order to get the second-order approximation. This procedure further carries on up to the level in which a convergent limit is obtained that signifies the real physical value of the fields. The convergence factor is additionally influenced by the size of the Yee cell cube is referred to as mesh size. In the present simulation, the mesh dimension is selected as x = 40 nm, y = 40 nm, z = 160 nm, with 0.45 nm step size applied in all of the three dimensions of the simulated region which is certainly seen to be sufficient enough to fulfil the convergence requirements. Cu is selected for the present simulation. The optical constants of Cu are obtained from the available publication [21]. Total Field Scatter Field (TFSF) is employed as a form of source of light which makes use of plane waves in the shape of a box with dimensions x= 360 nm, y = 360 nm, z = 140 nm in which the nanoparticle is totally fitted inside. One particular side of the box provides the incident light, propagation direction as well as polarization. This type of source of light is suitable for calculations which include the scattering phenomenon. To calculate the power absorbed by the nanoparticle, a total field monitor (with dimensions x= 330 nm, y= 330 nm, z = 120 nm) is positioned inside the TFSF source. On the other hand, a scattered field monitor (with dimensions x= 400 nm, y= 400 nm and z= 160 nm) is positioned outside the TFSF source in order to calculate the power scattered by the nanoparticle which is kept inside. The schematic of the simulated region is presented in figure 1. The incident plane wave is taken into consideration together with a polarization angle of 90^0 which usually signifies s-polarized radiation. The simulated data provided by the total as well as scattered field power monitors assist to calculate the extinction coefficient that implies the overall loss of the energy from the incident wave as a result of absorption and scattering respectively. The power absorbed by the nanoparticle is calculated by summing up the contributions from all the sides of the total field monitor cube. The scattering monitor provides the scattered power associated with the inside structure because, at the TFSF boundaries, the resultant power is obtained by subtracting the power absorbed from the incident waves. Figure 2 (a), and 2 (b), indicate the cross-sectional view and 3-D view of the overall geometry. An ellipsoid geometrical structure is designed with axes dimension x= 10 nm, y= 10 and z= 20 nm. The primary reason for selecting ellipsoid geometry is due to the fact that this type of particular structure provides acceptable results, which were found to be tally with the experimental outcomes [19]. To simulate the optical cross-sections, FDTD simulation volume is defined at first. Both the symmetric and antisymmetric as well as perfectly matched layers (PML) boundary conditions are applied along the x, y and z-axis respectively so that it saves the computational time required for the simulation. The size of the FDTD model volume is considered adequately large (2000 nm in x, y and z directions located at the origin) to ensure the

simulated nanoparticle doesn't interact with the evanescent fields. The reason for selecting the larger FDTD spaces is to ensure that the size of the FDTD simulation space doesn't impact the absorption as well as scattering spectra. The mesh is generated in the areas in which the refractive index changes instantly or the geometries are small.

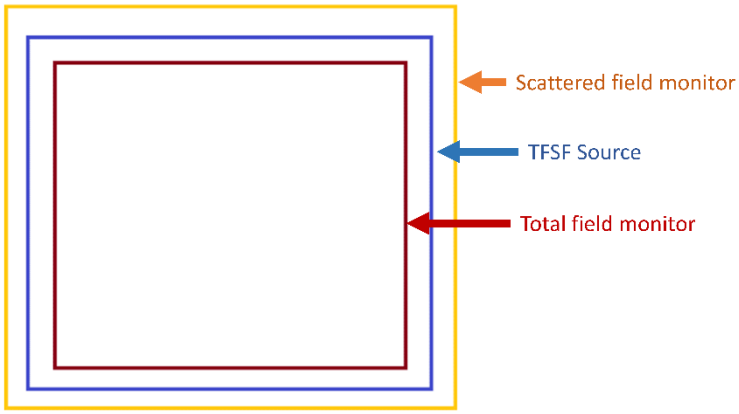

Figure 1: Schematic of the simulated region

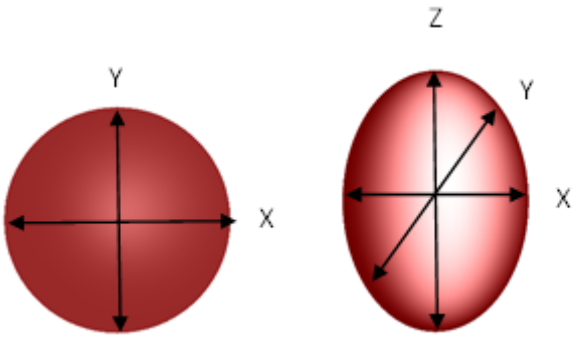

(a) (b)

Figure 2: The geometrical structure shows (a) a cross-sectional view and (b) a three-dimensional view of the design geometry.

Initially, the optical cross-sections and field intensities of a single Cu nanoparticle are computed by considering the diameter along x=10, y=10 and z=20 nm. To increase the size of the ellipsoid nanoparticle the diameter is further increased with a step size of 4 nm along the x, y and z axes and five numbers of particles (1st (14 nm, 14 nm, 24nm); 2nd (18 nm, 18 nm, 28nm); 3rd (22 nm, 22 nm, 32 nm); 4th (26 nm, 26 nm, 36 nm); 5th (30 nm, 30 nm, 40 nm)) have been designed.

3. Simulation results and discussion:

Figure 3 represents the optical absorption, scattering, and extinction cross-sectional spectra of a single Cu nanoparticle having 20 nm particle size. The result shows almost negligible scattering due to small particle size as compared to the wavelength of incident radiation. Because of the negligible scattering, both absorption and extinction spectra are found to be overlapped with each other. The spectrum reveals that in the visible range Cu shows an absorption peak as a result of the plasmon excitation of electrons when they are excited with the 530 nm wavelength. However, the amplitude of the LSPR resonance in Cu is not sharp as compared to the other noble metal (i.e silver) NPs. In the case of Cu, the interband transitions overlap with plasmon resonances which leads to the damping effect that minimizes the optical response at a given wavelength. This damping phenomenon is not found in silver because in the case of silver the interband transitions exist at much shorter wavelengths and do not overlap with the plasmon excitation [22]. Therefore, to increase the amplitude of the plasmon peak the particle size needs to be increased. Figure 4 shows the variation of the absorption with respect to the wavelength. As particle size increases from 20 nm to 40 nm, the excited resonant wavelength also shifted from 530nm to 550 nm wavelength. The redshift is observed because of the size dependent properties of the LSPR. Figure 5 shows the enhancement of absorption cross-section with respect to the particle size variation. A non-linear increment is found to be observed and the absorption cross-section increases from ~ 9.16 $x10^{-6}$ μm^2 to 2.32 x 10^{-4} μm^2 when the particle size increases from 20 nm to 40 nm respectively.

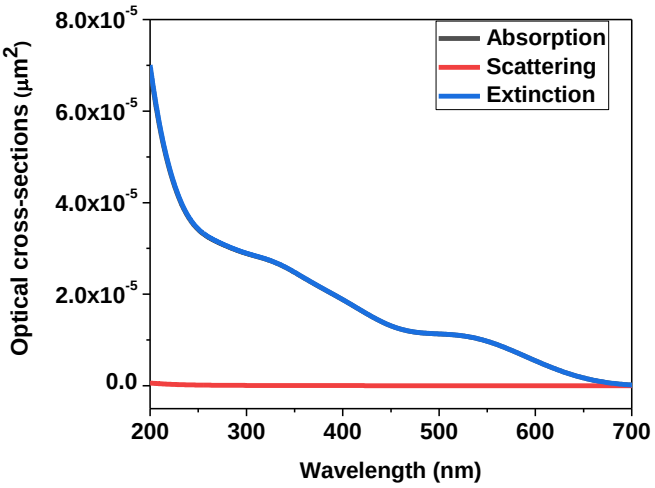

Figure 3: Optical spectra of Cu nanoparticle

Figure 6 reflects the size-dependent scattering spectra of the Cu nanoparticle, which signifies that the scattering is almost negligible when the particle size is increased from 20 nm to 28 nm. However, when the size is further increased beyond 28 nm, a significant scattering is observed. In this case, the scattering is found to be highest at the lower wavelength in the UV range, on the other hand, its magnitude decreases and attains a minimum at the higher wavelength. The decreasing scattering cross-section at the higher wavelength is due to the fact that for particle size less than the wavelength of incident radiation, the scattering is inversely proportional to the 4th order of the wavelength [23]. In figure 7, the variation of extinction cross-sectional spectra ($\sigma_{Extinction}$), which is the sum of the cross-sections of absorption ($\sigma_{Absorption}$) and scattering ($\sigma_{Scattering}$) of light which is calculated by the relationship [24].

$$\sigma_{Extinction} = \sigma_{Absorption} + \sigma_{Scattering} \quad (1)$$

The study of extinction spectra reveals that the absorption contribution toward the total extinction cross-section is more dominant than compared to scattering due to its higher order of absorption. In the transmission spectra provided in figure 8, show that smaller particle highly transmits the incident radiation as compared to the larger particle. All the nanostructures exhibit a strong transmission minimum at the wavelength close to 590 nm in the visible spectrum. However, above 600 nm, these nanostructures exhibit an increasing trend of transmission.

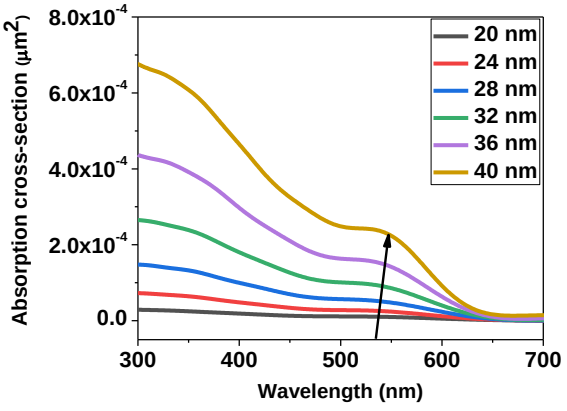

Figure 4: Shifting of absorption peak with respect to wavelength.

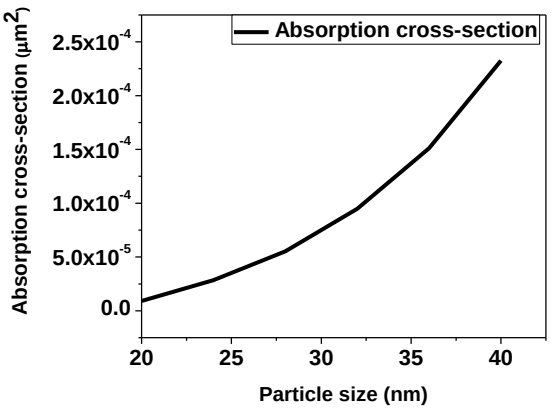

Figure 5: Enhancement of absorption with respect to the particle size variation

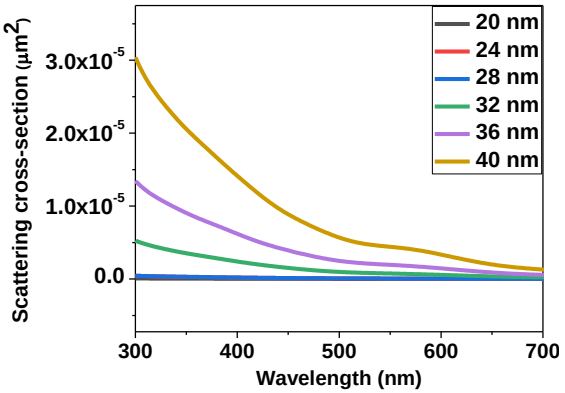

Figure 6: Scattering spectra with respect to the wavelength.

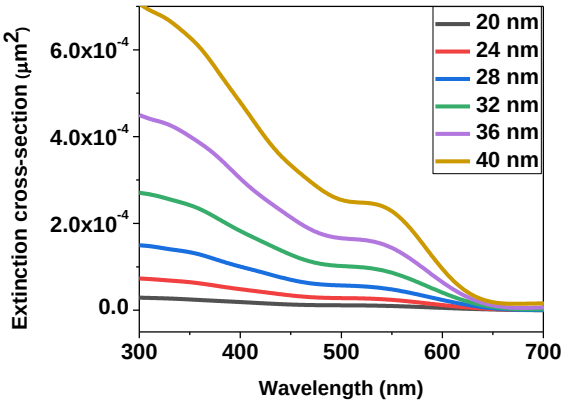

Figure 7: Extinction spectra with respect to the wavelength

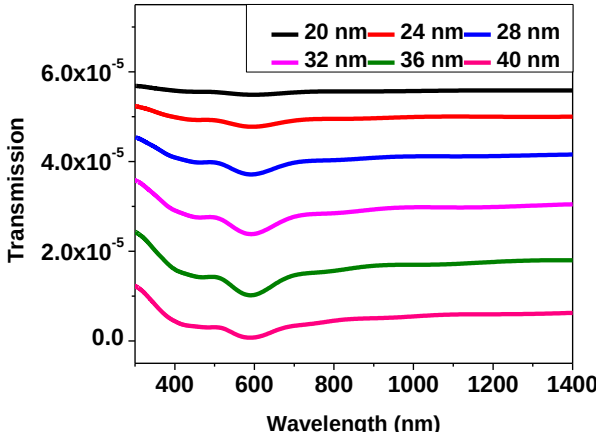

Figure 8: Transmission with respect to the particle size variation.

The variation of electric as well as magnetic field intensities at different particle sizes is also simulated and provided in Table 1 and Table 2 respectively. When metallic nanoparticle (whose size is less than the wavelength of incident radiation) interacts with electromagnetic radiations, LSPR primarily constrains the light energy into the surfaces of the metals in the form of electromagnetic fields with the highest field intensities found on the surface. From Table 1, it is observed that Cu nanoparticle having a particle size of 40 nm exhibits the highest electric field intensity in almost the entire wavelength as compared to the other sizes. The field intensity increases from 8.89 $(V/m)^2$ at 300 nm wavelength to the highest magnitude between 500 to 600 nm (~ 16.9) $(V/m)^2$. However, it is observed that the field intensity gradually drops down to 12.2 $(V/m)^2$ at the higher wavelength (700 nm). The highest electric field intensity in the visible range between 500 to 600 nm arises because of the strong coherent collective oscillation of the conduction electrons due to surface plasmon resonance. Above 600 nm wavelength, the field intensity decreases because at that wavelength the resonance condition is not satisfied. As far as the magnetic field intensity is concerned (Table 2), it is observed that at a given wavelength, the field intensity increases as the particle size increases. Cu nanoparticle having 40 nm size exhibits the highest magnetic field intensity (~ 7.74 x 10-6 $(A/m)^2$) at 300 nm wavelength. However, the order of magnitude is far lower than the electric field intensity at that particular wavelength. At the longer wavelength, the field intensity decreases. Figure 9 shows the visualization of local electric field intensity in the vicinity of the Cu nanoparticle having 40 nm particle size as a function of wavelength. The strong electric field arises from the upper and lower surface of the nanoparticle due to the s-polarization nature of the incident wave.

Table 1 Distribution of electric field intensity ($|E|^2$) in $(V/m)^2$ associated with the particle size variation from 20 to 40 nm

Sl No	Wavelength (nm)	E_{20}	E_{24}	E_{28}	E_{32}	E_{36}	E_{40}
1	300	5.15	6.27	6.69	7.77	7.97	8.89
2	400	6.91	8.2	8.92	10.5	10.9	12.4
3	500	7.35	8.33	9	10.6	10.8	13
4	600	8.98	9.63	10.6	12.4	13	16.8
5	700	7.32	7.84	8.4	9.74	9.95	12.2

Table 2 Distribution of magnetic field intensity ($|H|^2$) in $(A/m)^2$ associated with the particle size variation from 20 to 40 nm

Sl No	Wavelength	H_{20} ($x10^{-6}$)	H_{24} ($x10^{-6}$)	H_{28} ($x10^{-6}$)	H_{32} ($x10^{-6}$)	H_{36} ($x10^{-6}$)	H_{40} ($x10^{-6}$)
1	300	7.14	7.22	7.3	7.4	7.55	7.74
2	400	7.12	7.19	7.25	7.34	7.43	7.54
3	500	7.1	7.15	7.2	7.27	7.33	7.43
4	600	7.1	7.14	7.18	7.24	7.3	7.39
5	700	7.1	7.14	7.18	7.24	7.3	7.38

The highest absorption cross-section of Cu at 40 nm particle size in the visible range gives rise to the highest electric field intensity 16.9 (V/m)2 within 500 to 600 nm visible wavelength.

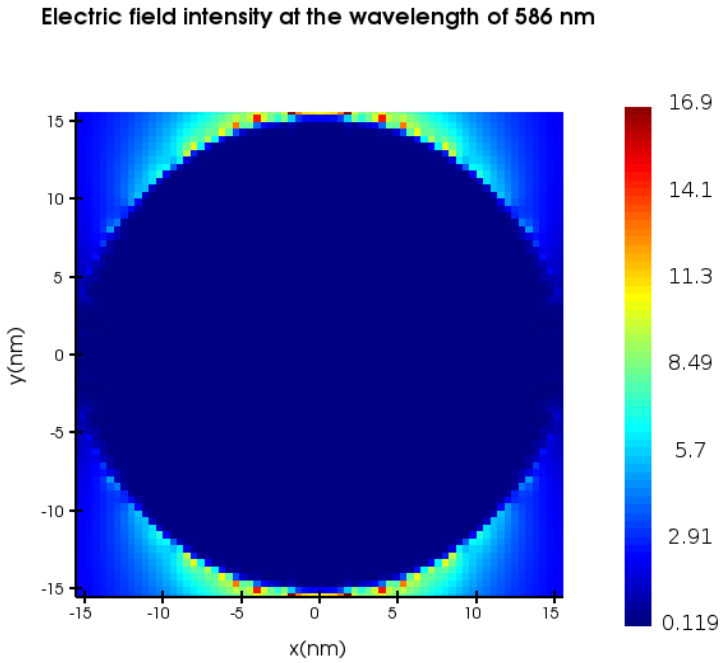

Figure 9: Distribution of electric field intensity

4. Conclusion:

Here, we have investigated the absorption, scattering, extinction and transmission spectra as well as field intensities of ellipsoid Cu nanoparticles. Our investigations demonstrate that particle size variation plays a very important role in the high absorption and high electric field intensities. A nonlinear enhancement is observed in the absorption spectra when the particle size is linearly varied from 20 to 40 nm. Moreover, FDTD simulations identify higher values of the electric field intensities which provide extraordinary enhancement when excited at

the designed resonant wavelength. The nanoparticle size variation provides tunability of the resonant peaks up to a particular excitation wavelength simply by adjusting its dimension. Our results conclude that particle size is an important parameter to understand the control enhancement of the optical properties and field intensities. The extraordinary enhancement of optical and field intensities of larger nanoparticles makes them good candidates for optoelectronics, light-harvesting applications etc.

Acknowledgement:

The authors would like to extend their sincere acknowledgement to IASST, Guwahati and the Department of Science and Technology, Government of India, for providing the computing facility for the simulation. One of the authors (Samir Thakur) would also like to acknowledge the Dept. of Applied Sciences, Gauhati University for their generous support.

References:

[1] D. Y. Lei, A. I. Fernández-Domínguez, Y. Sonnefraud, K. Appavoo, R. F. Haglund, J. B. Pendry, and S. A. Maier, ACS Nano 6, 1380, 2012.
[2] S. Mubeen, S. Zhang, N. Kim, S. Lee, S. Krämer, H. Xu, and M. Moskovits, Nano Lett. 12, 2088, 2012.
[3] L. Li, T. Hutter, U. Steiner, and S. Mahajan, Analyst 138, 4574, 2013.
[4] J. Zhao, A. Das, X. Zhang, G. C. Schatz, S. G. Sligar, and R. P. Van Duyne, J. Am. Chem. Soc. 128, 11004, 2006.
[5] S. A. Maier, M. L. Brongersma, P. G. Kik, S. Meltzer, A. A. G. Requicha, and H. A. Atwater, Adv. Mater. 13, 1501, 2001.
[6] R. Elghanian, J. J. Storhoff, R. C. Mucic, R. L. Letsinger, and C. A. Mirkin, Science 277, 1078, 1997.
[7] C. Loo, A. Lowery, N. Halas, J. West, and R. Drezek, Nano Lett. 5, 709, 2005.
[8] A. Ahmadivand and N. Pala, Appl Spectrosc 69, 277, 2015.
[9] S. Link and M. A. El-Sayed, J. Phys. Chem. B 103, 4212, 1999.
[10] S. Panigrahi, S. Kundu, S. K. Ghosh, S. Nath, S. Praharaj, S. Basu, and T. Pal, Polyhedron 25, 1263, 2006.
[11] J. A. Creighton and D. G. Eadon, J. Chem. Soc., Faraday Trans. 87, 3881, 1991.
[12] D. E. Eastman, Phys. Rev. B 2, 1, 1970.
[13] Y. Lin, Z. Chen, L. Fang, M. Meng, Z. Liu, Y. Di, W. Cai, S. Huang, and Z. Gan, Nanotechnology 30, 015402, 2019.
[14] J. Katyal and V. badoni, Materials Today: Proceedings 44, 5012, 2021.
[15] G. Singh, J. S. Sekhon, and S. S. Verma, in 13th International Conference on Fiber Optics and Photonics 2016, Kharagpur, 2016).
[16] G. Mie, Ann. Phys. 330, 377, 1908.
[17] IEEE Trans. Antennas Propagat. 14, 302, 1966.
[18] https://www.lumerical.com.
[19] S. Podder, J. Bora, S. Thakur, D. Gogoi, B. Basumatary, S. M. Borah, N. C. Adhikary, and A. R. Pal, Materials Chemistry and Physics 275, 125290, 2022.
[20] B. Basumatary, S. Podder, S. Thakur, J. Bora, B. Sharma, S. M. Borah, N. Ch. Adhikary, D. S. Patil, and A. R. Pal, ACS Omega 7, 7662, 2022.
[21] H. J. Hagemann, W. Gudat, and C. Kunz, J. Opt. Soc. Am. 65, 742, 1975.
[22] E. Kazuma, T. Yamaguchi, N. Sakai, and T. Tatsuma, Nanoscale 3, 3641, 2011.
[23] C. F. Bohren and D. R. Huffman, Absorption and Scattering of Light by Small Particles, 1st ed., Wiley, 1998.
[24] A. D. Kondorskiy, N. T. Lam, and V. S. Lebedev, J Russ Laser Res 39, 56, 2018.